Mode of Action for Linear Peptide Inhibitors of HIV-1 gp120 Interactions[†]

Alyssa C. Biorn,[‡,§,||] Simon Cocklin,[‡,§] Navid Madani,[§,⊥] Zhihai Si,[⊥] Tijana Ivanovic,[⊥] James Samanen,[@] Donald I. Van Ryk,[‡,#] Ralph Pantophlet,[+] Dennis R. Burton,[+] Ernesto Freire,[●] Joseph Sodroski,[⊥] and Irwin M. Chaiken*,[‡]

Department of Biochemistry, Drexel University College of Medicine, Philadelphia, Pennsylvania 19102, Division of Human Retrovirology, Dana-Farber Cancer Institute, Department of Pathology, Division of AIDS, Harvard Medical School, and Department of Cancer Biology, Harvard School of Public Health, Boston, Massachusetts 02115, GlaxoSmithKline, King of Prussia, Pennsylvania 19406, Department of Biology, Johns Hopkins University, Baltimore, Maryland 21218, and Departments of Immunology and Molecular Biology, The Scripps Research Institute, La Jolla, California 92037

ABSTRACT: The linear peptide 12p1 (RINNIPWSEAMM) was previously isolated from a phage display library and was found to inhibit interaction of HIV-1 gp120 with both CD4 and a CCR5 surrogate, mAb 17b [Ferrer, M., and Harrison, S. (1999) *J. Virol. 73*, 5795−5802]. In this work, we investigated the mechanism that leads to this dual inhibition of gp120 binding. We found that there is a direct interaction of 12p1 with gp120, which occurs with a binding stoichiometry of 1:1. The peptide inhibits binding of monomeric YU2 gp120 to both sCD4 and 17b at IC_{50} values of 1.1 and 1.6 μM, respectively. The 12p1 peptide also inhibited the binding of these ligands to trimeric envelope glycoproteins, blocked the binding of gp120 to the native coreceptor CCR5, and specifically inhibited HIV-1 infection of target cells in vitro. Analyses of sCD4 saturation of monomeric gp120 in the presence or absence of a fixed concentration of peptide suggest that 12p1 suppression of CD4 binding to gp120 is due to allosteric inhibitory effects rather than competitive inhibition of CD4 binding. Using a panel of gp120 mutants that exhibit weakened inhibition by 12p1, the putative binding site of the peptide was mapped to a region immediately adjacent to, but distinguishable from, the CD4 binding footprint. In the case of the peptide, the effects of single-12p1 residue substitutions and various peptide truncations indicate that the side chain of Trp7 and other structural elements of 12p1 are critical for gp120 binding or efficient inhibition of binding of a ligand to gp120. Finally, 12p1 was unable to inhibit binding of sCD4 to a gp120 mutant that is believed to resemble the CD4-induced conformation of gp120. These results suggest that 12p1 preferentially binds gp120 prior to engagement of CD4; binding of the peptide to gp120 limits the interaction with ligands (CD4 and CCR5) that are generally crucial for viral entry. More importantly, these results indicate that 12p1 binds to a unique site that may prove to be a prototypic target for novel CD4−gp120 inhibitors.

The Joint United Nations Programme on HIV/AIDS[1] (UNAIDS) estimates that 42 million people were infected with HIV-1 as of the end of 2002, with 5 million newly infected persons and 3.1 million deaths in 2002. To combat this virus, multiple approaches must be taken; the seemingly few vulnerabilities of HIV may have to be targeted simultaneously to successfully prevent or inhibit viral infection and/or replication.

A primary target is the HIV envelope glycoprotein (Env). The Env spikes on the viral membrane are composed of a gp41 transmembrane trimer and three noncovalently associated gp120 surface glycoproteins. Viral infection is initiated by the interaction of gp120 with the extracellular portion of CD4 on the target cell. The binding of these two proteins promotes a conformational change in gp120 that increases its affinity for a cell surface coreceptor, usually CCR5. This second binding event leads to further conformational changes that culminate in the fusion of the viral and target cell membranes. Blocking the interactions between gp120 and cell surface receptors, then, is an attractive goal for preventing HIV infection.

The HIV-1 Env proteins, however, exhibit unusual features that influence their feasibility as a target. While there is currently no crystal structure of gp120 in the unbound state, calorimetric methods have determined that it undergoes a

* To whom correspondence should be addressed: Drexel University College of Medicine, 11102 New College Building, MS #497, 245 N. 15th St., Philadelphia, PA 19102. Phone: (215) 762-4197. Fax: (215) 762-4452. E-mail: imc23@drexel.edu.

[‡] Drexel University College of Medicine.

[§] These authors contributed equally to this work.

[||] Current address: Mayo Clinic, 200 First St. SW, Rochester, MN 55905.

[⊥] Dana-Farber Cancer Institute, Harvard Medical School, and Harvard School of Public Health.

[@] GlaxoSmithKline.

[#] Current address: National Institute of Allergy and Infectious Diseases, National Institutes of Health, 10 Center Dr., Rm. 6A-08, Bethesda, MD 20892.

[+] The Scripps Research Institute.

[●] Johns Hopkins University.

[1] Abbreviations: HIV, human immunodeficiency virus; AIDS, acquired immune deficiency syndrome; sCD4, soluble CD4; mAb, monoclonal antibody; ELISA, enzyme-linked immunosorbent assay; TMB, 3,3′,5,5′-tetramethylbenzidine; HRP, horseradish peroxidase; SPR, surface plasmon resonance.

large structural rearrangement upon binding of several of its ligands, especially CD4 and antibodies directed against receptor-binding regions (*1*). Monomeric gp120 has been proposed to be extremely flexible prior to binding; it has been suggested that the inner and outer domains of gp120 are mobile with respect to each other, and the bridging sheet that spans the two domains is unfolded (*2*). Thermodynamic analyses demonstrate that the binding of CD4 to gp120 causes an unusually large decrease in entropy, indicating significant ordering of the protein (*3*), and that this structural stabilization is propagated to other regions of the gp120 monomer, being initiated from the CD4 binding site (*1*). An inhibitor that could take advantage of the unusual flexibility of gp120 might be more effective than a traditional competitive inhibitor. If, for example, a small molecule could prevent gp120 from attaining conformations critical for entry, as has been seen for some CD4 binding site antibodies (*4*), it could inhibit either the binding of HIV-1 to its receptors or postreceptor binding events involved in fusion of the viral and target cell membranes.

Several small peptide mimetics of CD4 have been reported thus far to inhibit the binding of gp120 to CD4 (*1, 5, 6*). Most of these, however, have produced conformational changes in gp120 similar to those induced by CD4 and hence have led to activation, to a state with increased coreceptor affinity. In this way, these molecules are successful CD4 competitors, but potentially could facilitate, rather than inhibit, HIV-1 entry. A more successful inhibitor might not only inhibit CD4−gp120 binding but also either physically block the gp120−coreceptor interaction or prevent the activating conformational change that gp120 must undergo to efficiently bind CCR5.

Ferrer and Harrison (*7*) screened a random phage library of 12-mer peptides for candidates that would bind to gp120. They discovered a sequence, RINNIPWSEAMM (12p1), that bound to gp120 and inhibited its interaction not only with CD4 but also with 17b, an antibody that recognizes an epitope overlapping the CCR5 binding site. Here we extend this study with a number of goals: (a) to quantitate the degree of co-inhibition of CD4 and 17b binding, (b) to demonstrate the direct binding of the peptide to gp120 and determine its stoichiometry, (c) to determine which residues are critical for gp120 binding and ligand inhibition, (d) to determine the site of interaction on gp120, (e) to examine interaction of 12p1 with the Env trimer, including functional virion trimers, and (f) to investigate the influence of gp120 conformation on peptide binding. A variety of modifications and truncations of the parent 12p1 peptide were made to identify residues that are critical for binding gp120. The peptides were studied both with a biosensor for effects on monomeric gp120 binding and with an ELISA for effects on binding to stable gp120 trimers.

The results confirmed that 12p1 inhibits interaction of gp120 with both CD4 and 17b, as well as CCR5, and showed that its binding exhibits 1:1 stoichiometry at inhibitory concentrations. We found that several residues, especially Trp7, are critical for 12p1 inhibition of binding of gp120 to CD4 and 17b, and that truncation of the peptide also weakens its inhibitory effectiveness. We also investigated the mode of action of 12p1. The 12p1 peptide appears to bind an unactivated (CD4-unbound) conformation of gp120, resulting in noncompetitive inhibition of the binding of ligands that

induce or prefer the activated (CD4-bound) state. This suggests that limiting the ability of gp120 to assume an activated conformation may contribute to the mode of 12p1 inhibition of HIV-1 entry.

EXPERIMENTAL PROCEDURES

Peptide Synthesis and Purification. Peptides were initially obtained from American Peptide Co. (Sunnyvale, CA). These peptides were synthesized, purified by reverse phase HPLC (RP-HPLC), and validated by electrospray MS and amino acid analysis. We synthesized additional peptides using solid phase peptide synthesis on an Applied Biosystems 433A peptide synthesizer. Peptides were made at the 0.1 mmol scale on Rink amide resin using FastMoc synthesis, as described previously (*1*). Peptides were cleaved from the resin with 10 mL of trifluoroacetic acid, 0.5 mL of H_2O, 0.5 mL of ethanedithiol, and 0.25 mL of thioanisole for 2 h at room temperature (RT). Resin was filtered out, and the peptide was precipitated with cold ether. Dried, solid peptide was dissolved in 10% acetic acid and purified by RP-HPLC on a C18 preparative column (Vydac). The peak with the desired peptide was verified by MALDI-MS (performed at the Wistar Institute, Philadelphia, PA). HPLC fractions were lyophilized, and the solid peptide was dissolved in phosphate-buffered saline (PBS) at pH 7.4. The peptide concentration and amino acid composition were determined by amino acid analysis (performed at the Howard Hughes Medical Institute/ Keck Biotechnology Resource Laboratory, Yale University, New Haven, CT).

Biosensor Experiments. All surface plasmon resonance (SPR) experiments were performed on a BIA3000 optical biosensor (Biacore, Inc., Uppsala, Sweden), in a manner similar to that in previous studies (*1*). A CM5 sensor chip was derivatized by amine coupling with either the CD4 extracellular domain (sCD4), mAb 17b Fab, or gp120 YU2, using mAb 2B6R Fab (to IL-5 receptor α) as a control surface. For competition experiments, ligands were immobilized to a surface density of approximately 800−1000 RU. The indicated analytes were passed over the surfaces at a flow rate of 50 μL/min, for 2.5 min, followed by a 2 min dissociation phase. Surfaces were regenerated with 35 mM NaOH and 1.3 M NaCl for sCD4, and 10 mM HCl for 17b and 2B6R. For direct binding experiments with a YU2 gp120 surface (2000 RU), a flow rate of 5 μL/min was used, with a 5 min association phase and a 2 min dissociation phase. CD4 saturation analyses in the presence or absence of 100 μM 12p1 were performed on a YU2 gp120 surface (2400 RU). sCD4 or sCD4/12p1 analyte mixtures were injected over the YU2 gp120 surface at a rate of 5 μL/min for 5 min, followed by a 5 min dissociation phase. YU2 gp120 surfaces were regenerated with 35 mM NaOH and 1.3 M NaCl. Buffer injections and control surface binding were subtracted for all reported data. Experiments were performed twice in duplicate.

Biosensor Data Analysis. The initial rate (v_i) of binding of gp120 to either sCD4 or 17b in the presence or absence of peptide was determined during the period of the association phase from 6 to 21 s. The slope of that line (RU/s, v_i) at each peptide concentration was calculated using Biaeval 3.0 software (Biacore). The fraction of the v_i of gp120 binding in the presence versus absence of peptide was

determined for each peptide concentration. For determination of the IC_{50} of 12p1, these fractions were plotted against the log of the 12p1 concentration. Curves were fit using SigmaPlot (SPSS, Inc.), and the 12p1 concentration at which the v_i of gp120 binding was half of that without peptide was designated the IC_{50}. For direct binding of the peptide to gp120, Biaeval software was used to determine R_{eq} at equilibrium (during the period of the association phase from 285 to 295 s) for each peptide concentration. R_{eq} was plotted versus 12p1 concentration, and the software calculated R_{max} for 1:1 binding. R_{max} was estimated for comparison by performing the identical experiment with sCD4 and calculating R_{max} for 12p1 based on its mass difference with sCD4, as R_{max} is proportional to mass. Sensorgrams obtained from sCD4 saturation analyses also were fit to a 1:1 binding model using Biaeval software, and resultant R_{eq} values were plotted against sCD4 concentration. Saturation curves of R_{eq} versus sCD4 concentration in the presence or absence of 12p1 were then fitted against a 1:1 steady-state model to obtain equilibrium K_D values.

Effect of the Peptide on gp120−Ligand Binding Measured with an ELISA. The ELISAs were conducted with soluble, stabilized sgp140Δ683(−/GCN4) trimers from the HxBc2 HIV-1 strain (8). These soluble envelope glycoprotein trimers have C-terminal C9 peptide and His$_6$ tags. The murine mAb 1D4, which is directed against the bovine rhodopsin C9 peptide, was immobilized on the ELISA plate at 4 °C overnight. After the plates had been blocked and washed, the soluble HIV-1 envelope glycoprotein trimers were captured on the plate. Biotinylated soluble sCD4 (0.5 µg/mL) was then added to the plate in the presence of increasing concentrations of peptide (0, 12.5, 50, and 200 µM) for 1 h at RT. This was followed by washing and addition of avidin-bound HRP at a 1:45000 dilution for 1 h at RT. To determine peptide competition with a panel of human anti-gp120 mAbs, 100 µM peptide and 0.5 µg/mL antibody (1:2000 dilution) were added to the immobilized trimers of wild-type or mutant HxBc2 gp120 simultaneously and incubated for 1 h. An HRP-conjugated goat anti-human antibody (1:5000) was next added to the bound antibody. The extent of HRP conjugate binding was detected in both assays with 100 µL of TMB substrate (KPL, Gaithersburg, MD). The reaction was stopped by adding 100 µL of 1 N HCl, and the OD was measured at 450 nm with a microplate reader.

CCR5 Binding Assay. To determine if peptides could inhibit binding of gp120 to CCR5 independent of CD4 interactions, 500 µL of crude cell supernatant containing monomeric ADA ΔV1/V2 gp120, metabolically labeled with [^{35}S]Cys/Met, was first incubated in the presence or absence of peptide (100 µM) at RT for 1 h. This mixture was then added to Cf2Th-CCR5 target cells, and the cells were incubated at 37 °C for 2 h. After being washed, the cells were lysed, and the bound proteins were precipitated with a mixture of sera from HIV-1-infected individuals and separated by SDS−PAGE. The precipitated labeled ADA ΔV1/V2 gp120 was visualized by autoradiography and quantitated using the Storm 820 imaging system (Molecular Dynamics).

Viral Inhibition Assay. To determine if peptide 12p1 inhibits infection of cells by virus, viral inhibition assays were performed. 293T human embryonic kidney cells and Cf2Th canine thymocytes (ATCC) were grown at 37 °C and 5% CO_2 in Dulbecco's modified Eagle's medium (Invitro-

Table 1: Sequence Alignment of 12p1 and Variant Peptides vs CD4

12p1	R	I	N	N	I	P	W	S	E	A	M	M
[R1A]12p1	**A**	I	N	N	I	P	W	S	E	A	M	M
[R1K]12p1	**K**	I	N	N	I	P	W	S	E	A	M	M
[I5dA]12p1	R	I	N	N	**DA**	P	W	S	E	A	M	M
[W7F]12p1	R	I	N	N	I	P	**F**	S	E	A	M	M
12p1(1-10)	R	I	N	N	I	P	W	S	E	A	___	
12p1(1-8)	R	I	N	N	I	P	W	S	_____			
[R1A]12p1(1-8)	**A**	I	N	N	I	P	W	S	_____			
12p1(2-8)	_	I	N	N	I	P	W	S	_____			
CD4 (F43 underlined)	^{49}S	P	G	K	T	L	**F**	S	G	Q	N	G^{38}

gen) containing 10% fetal bovine serum (Sigma) and 100 µg/mL penicillin-streptomycin (Mediatech, Inc.). Cf2Th cells stably expressing human CD4 and CCR5 or CXCR4 (9) were grown in medium supplemented with 0.4 mg/mL G418 (Invitrogen) and 0.15 mg/mL hygromycin B (Roche Diagnostics). 293T cells were cotransfected with vectors expressing the pCMVΔP1Δenv HIV Gag-Pol packaging construct (10), the envelope glycoproteins of vesicular stomatitus virus (VSV) or HIV-1 isolates (ADA, JR-CSF, YU2, or HxBc2), and a firefly luciferase reporter gene, at a DNA ratio of 1:1:3 (micrograms) using Effectene transfection reagent (Qiagen). Cotransfection produced single-round, replication-defective viruses. The virus-containing supernatants were harvested 24−30 h after transfection, filtered (0.45 µm), aliquoted, and frozen at −80 °C until further use. The reverse transcriptase activities of all viruses were measured as described previously (11). To determine infection by single-round luciferase viruses, Cf2Th-CD4-CCR5/CXCR4 target cells were seeded at a density of 6×10^3 cells/well in 96-well luminometer-compatible tissue culture plates (Dynex) 24 h before infection. On the day of infection, the 12p1 peptide (0.3−300 µM) was added to recombinant viruses (10 000 reverse transcriptase units) to a final volume of 50 µL and incubated at 37 °C for 30 min. The medium was then removed from the target cells, which were then incubated with the virus/peptide mixture for 48 h at 37 °C. The medium was removed from each well, and the cells were lysed with 30 µL of passive lysis buffer (Promega) and by three freeze−thaw cycles. An EG&G Berthold LB 96V microplate luminometer was used to measure luciferase activity of each well after the addition of 100 µL of luciferin buffer [15 mM $MgSO_4$, 15 mM KPO_4 (pH 7.8), 1 mM ATP, and 1 mM dithiothreitol] and 50 µL of 1 mM d-luciferin potassium salt (BD Pharmingen).

RESULTS

Peptide 12p1 Inhibits Binding of YU2 gp120 to both CD4 and 17b. It has been previously shown that peptide 12p1 (sequence shown in Table 1) inhibits the binding of gp120 to CD4 (by ELISA) and 17b (by SPR) (7). We sought to establish a quantitative assay for determining the extent of inhibition by 12p1 and variant peptides. To assess the inhibition of binding of gp120 to CD4 and 17b, we examined
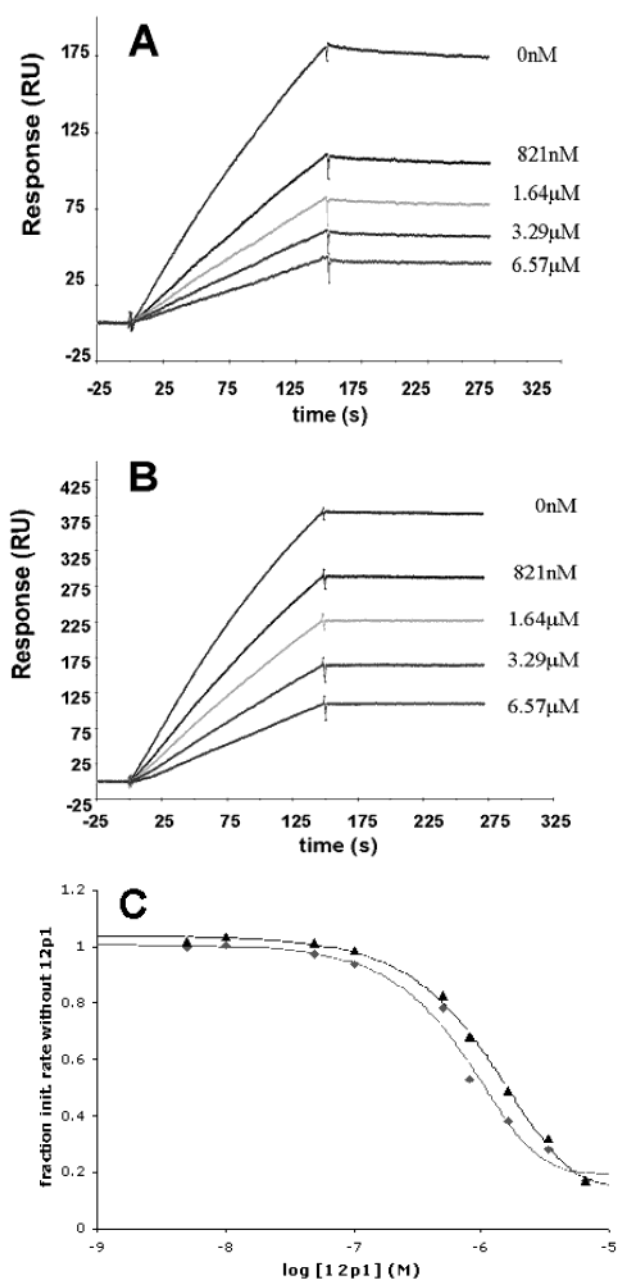
FIGURE 1: Peptide 12p1 inhibition of binding of gp120 to CD4 and 17b. CD4 (A) and 17b (B) were immobilized on a CM5 sensor chip in a BIA3000 instrument. YU2 gp120 (50 nM) was passed over each surface in the absence (0 nM) or presence of 821 nM to 6.57 μM 12p1. Buffer injections and control surface binding have been subtracted to obtain all curves. Experiments were repeated twice in duplicate with similar results. Data from one experiment are shown. (C) Log plot for determining IC$_{50}$ for 12p1 inhibition of binding of gp120 to CD4 ($\blacklozenge$) and 17b ($\blacktriangle$). Curves were fit using SigmaPlot, and the 12p1 concentration at which the initial rate of gp120 binding was half of that without peptide was designated the IC$_{50}$.

the interactions by surface plasmon resonance (SPR) using a Biacore 3000 instrument. The analyte, YU2 gp120 (50 nM) in the absence or presence of increasing amounts of peptide, was passed over immobilized sCD4, 17b Fab, and control 2B6R Fab. Under the conditions that were used, 12p1 exhibited no direct binding to either sCD4 or 17b (data not shown). As shown in Figure 1, increasing concentrations of 12p1 significantly inhibited the binding of YU2 to both sCD4
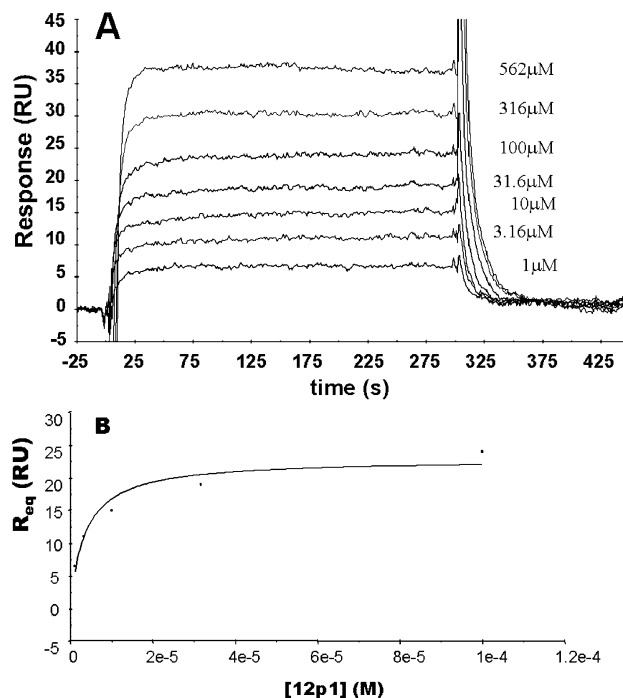

FIGURE 2: Direct binding of 12p1 to immobilized gp120. (A) Response curves for increasing concentrations of 12p1 binding to immobilized YU2 gp120. (B) Fit of direct binding data to a steady-state 1:1 binding model. R_{eq} was calculated from 285 to 295 s from each curve in panel A and plotted vs 12p1 concentration. Equilibrium binding constants for the YU2$-$12p1 interaction are as follows: $K_A = 2.74 \times 10^5$ M^{-1} and $K_D = 3.65$ μM.

(Figure 1A) and 17b (Figure 1B) surfaces. The fraction of the initial rate of YU2 binding in the presence or absence of peptide (taken to be 1.0) was determined for each peptide concentration and plotted as a function of the log of the peptide concentration (Figure 1C). Using SigmaPlot software, the IC$_{50}$ values for 12p1 inhibition of binding of gp120 to sCD4 and 17b were determined to be 1.1 and 1.6 μM, respectively. The value for sCD4 inhibition is more than 20-fold lower than that reported by Ferrer and Harrison for HxBc2 gp120 (as measured with an ELISA), but is in line with the values reported for strains SF2 and ADA (*7*).

Peptide 12p1 Binds Directly to YU2 gp120. We next used SPR to verify that 12p1 binds directly to gp120 and to determine the binding stoichiometry at the peptide's effective concentration. Increasing concentrations of 12p1 were passed over a high-density (2000 RU) YU2 gp120 surface (Figure 2A). The binding data fit to those expected of a bimolecular binding process with a K_D of 3.7 μM (Figure 2B). Using sCD4 as a standard, the expected R_{max} for 12p1, assuming 1:1 binding, was 26.7 RU. Although the response for peptide binding exceeded 30 RU at the highest 12p1 concentrations, the R_{max} at 100 μM peptide (roughly 30-fold greater than K_D) did not exceed the expected stoichiometric value. Therefore, we believe that the effect of the peptide is a result of 1:1 peptide$-$gp120 binding and not of an aggregation of the peptide, or of the peptide binding to multiple sites on gp120.

Using this same high-density YU2 gp120 surface, we confirmed the inhibition of gp120$-$CD4 binding in the reverse orientation compared with that in Figure 1A. Figure 3 shows the inhibition of binding of sCD4 to surface-immobilized YU2 gp120 by increasing concentrations of
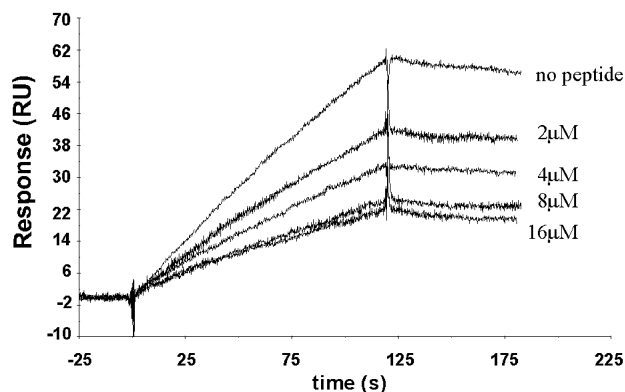
FIGURE 3: 12p1 competition with CD4 for binding to immobilized gp120. CD4 (10 nM) was passed over a high-density YU2 gp120 surface at a rate of 30 μL/min in the absence (no peptide) or presence of 2−16 μM 12p1.
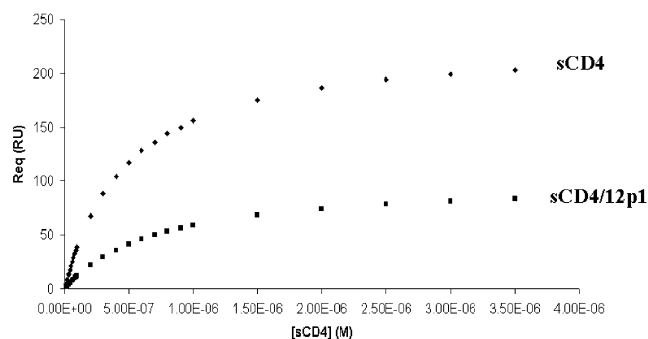

FIGURE 4: Analysis of sCD4 saturation of YU2 gp120 in the presence and absence of 12p1. R_{eq} values were obtained from fitting sensorgrams charting the response of immobilized YU2 to increasing concentrations of CD4 (0−3.5 μM) in the presence or absence of 100 μM 12p1. The resultant R_{eq} responses were then plotted vs sCD4 concentration and fitted to a steady-state 1:1 binding model to obtain equilibrium binding constants K_A and K_D. Under the conditions that were used, the presence of 12p1 had no discernible effect on the kinetics of interaction between YU2 and sCD4 (K_D values of 721 and 429 nM in the presence and absence of the peptide, respectively) but had a marked effect on the total amount of sCD4 bound by YU2.

12p1. In addition to buffer and control surface subtraction, the binding of peptide alone at each concentration has been subtracted from the corresponding curve plus sCD4. 12p1 clearly inhibits gp120−CD4 binding with either gp120 or sCD4 immobilized.

Peptide 12p1 Inhibition Follows an Allosteric Mode. We investigated the mode of inhibition of binding of CD4 to gp120 by 12p1 via biosensor experiments. Soluble four-domain CD4 (ImmunoDiagnostics, Inc.), in the range of 0−3.5 μM, was passed over a high-density YU2 gp120 surface (2400 RU) in the presence or absence of 100 μM 12p1 peptide. The resultant sensorgrams were analyzed using Biaeval 3.0 and fitted to a 1:1 binding model. From the fitted data, the predicted responses at equilibrium (R_{eq}) were plotted against the concentration of sCD4 analyte to generate saturation curves, which are shown in Figure 4. In the absence of the 12p1 peptide, an experimental maximum for sCD4 binding of approximately 200 RU was reached. However, this maximum response was decreased to only 85 RU in the presence of 100 μM peptide. For an inhibitor that operates competitively, it would be expected that its inhibitory effect should be negated at sufficiently high substrate

(sCD4) concentrations. This is not the case with 12p1, however, with the binding capacity of sCD4 for gp120 being reduced similarly over a wide range of sCD4 concentrations. This is typically indicative of a noncompetitive, allosteric effect. In addition, the saturation curves were fitted to a 1:1 steady state binding model to determine the K_D with and without peptide. Under the conditions outlined in Experimental Procedures, the gp120−sCD4 interaction had an apparent equilibrium dissociation constant of 429 nM. In the presence of the peptide, the K_D was 721 nM. Our results, including both Figure 4 and the sensorgrams (not shown) from which they were obtained, show that the affinity of observed gp120−sCD4 interaction remains the same when 12p1 is present and that it is the overall binding capacity of the gp120 surface that is reduced. This argues for a mode of action of 12p1 in which the peptide binds to and stabilizes a form of gp120 that is not competent to bind CD4.

Variants of 12p1 Have Reduced Inhibitory Activity. Ferrer and Harrison previously determined, through Ala scanning mutations of 12p1, that the peptide sequence was important for its inhibitory activity (7). Replacement of any of the interior residues (NNIPWS) was especially detrimental to peptide inhibitory function. The effect of sequence was explored further by synthesizing a number of variants of peptide 12p1 (Table 1). Peptides were tested for their abilities to inhibit gp120 binding as described above for 12p1. All of the variations had effects on the inhibitory abilities of the peptides, to differing extents. Two peptides, [I5dA]12p1 and [W7F]12p1, showed no significant inhibitory activity toward either sCD4 or 17b binding at concentrations of up to 125 μM (data not shown). Other peptides that had truncations from either the N- or C-terminus, or that contained altered residues closer to either terminus, were still able to inhibit gp120−CD4 or −17b binding, although with reduced apparent affinities (Figure 5). Peptides 12p1(1−10), 12p1(1−8), 12p1(2−8), and [R1A]12p1 (panels A−D of Figure 5, respectively) retained inhibitory activity against 17b− and sCD4−gp120 binding, but only at much higher concentrations compared with 12p1. The initial rates in the presence of each peptide were approximately half that of gp120 alone at 25, 68.9, 100, and 69 μM, respectively. In each case, the ratio of sCD4 to 17b inhibition at every peptide concentration is very close to 1, similar to the pattern of inhibition observed for 12p1. These data indicate that sequence elements spanning the entire peptide contribute to inhibitory activity.

We then investigated whether the lack of inhibition of binding of gp120 by peptides [I5dA]12p1 and [W7F]12p1 was due to an inability to bind to gp120. High concentrations of the two different peptides were used as the analyte with the high-density YU2 gp120 surface, as described above for 12p1. Both peptides were able to bind to gp120, but only at concentrations much higher than those of the other peptides, and much higher than the concentrations at which they were tested in the inhibition assays (not shown). For example, at 1.76 mM, 1000-fold higher than the IC_{50} of 12p1, the R_{max} for binding of [I5dA]12p1 to gp120 was only approximately half of the value expected for 1:1 stoichiometry. It is likely, then, that the peptides' lack of inhibition of gp120 binding is due to their severely reduced affinities for gp120.

Effects of the Peptide on Trimeric Envelope Glycoprotein Interactions. Because gp120 exists on the virus as a trimer,
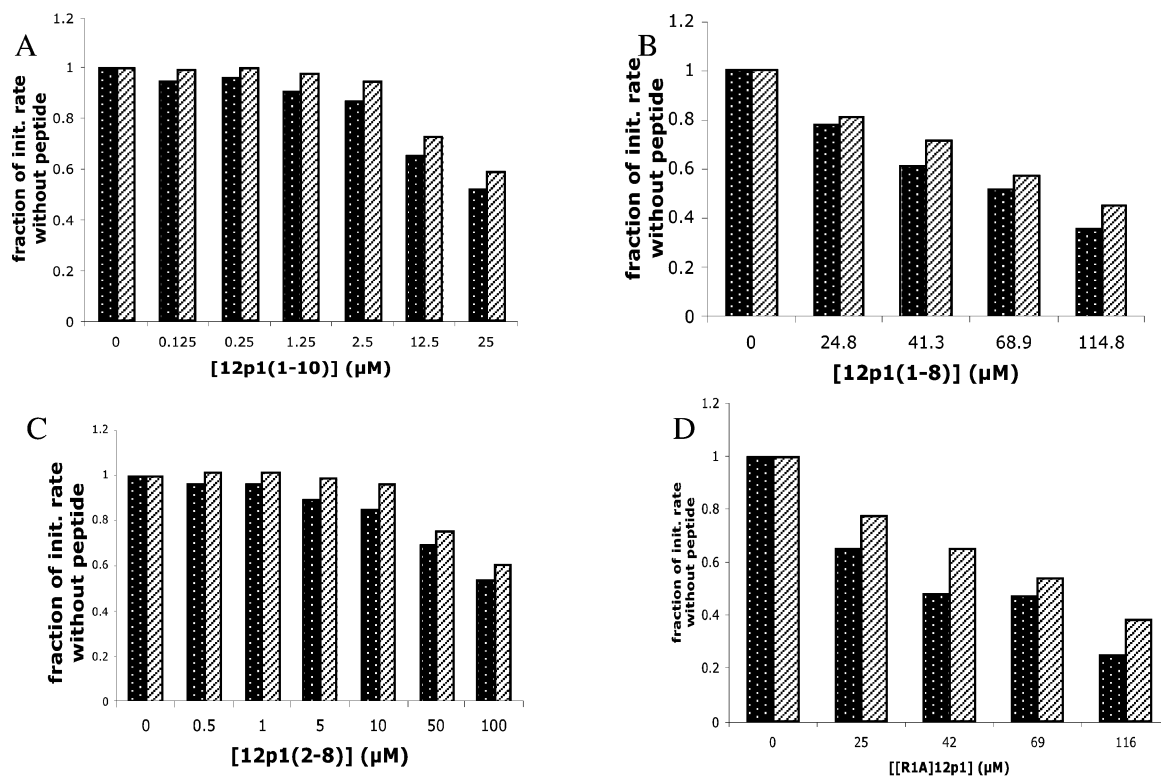
FIGURE 5: Inhibition of binding of gp120 to sCD4 and 17b by peptide variants. Increasing concentrations of peptides 12p1(1−10) (A), 12p1(1−8) (B), 12p1(2−8) (C), and [R1A]12p1 (D) were incubated with 50 nM YU2 gp120, and then the mixtures were passed over sCD4 (dark bars) and 17b (light bars) biosensor surfaces. The initial rate (v_i) of gp120 binding was determined for each peptide concentration. The fraction of v_i at each peptide concentration vs the v_i of gp120 alone is reported.

we sought to test the inhibitory effectiveness of 12p1 with this more naturally relevant form of gp120. For the ELISA-based assays, soluble, stabilized HIV-1 envelope glycoprotein trimers (HxBc2 strain) were captured on the plate via an immobilized antibody to their C-terminal C9 peptide tags. Peptide competition for the binding of biotinylated sCD4 was assessed. As shown in Figure 6A, the peptides had similar effects on envelope glycoprotein trimer−CD4 binding as they did on monomeric gp120 binding in the biosensor analyses. Peptide 12p1 was the most potent inhibitor, followed by 12p1(1−10) and the other truncated peptides. As in the biosensor assays, [I5dA]12p1 and [W7F]12p1 did not inhibit binding of CD4 to the envelope glycoprotein trimers. An additional peptide, [W7A]12p1, also did not inhibit the trimer−CD4 interaction. These results are consistent with those from the biosensor assays.

The group of peptides also was tested for their effects on sCD4 binding to a mutant envelope glycoprotein trimer with an alteration in gp120, S375W. This gp120 mutant was designed with the intention of filling the cavity that is partially occupied by Phe43 of CD4 in the gp120−CD4 complex (*12, 13*). The S375W change appears to promote a gp120 conformation that resembles the activated, CD4-bound, state (*13*). Previous studies have shown that this mutant binds sCD4 more readily than wild-type gp120 and shows a slight increase in the level of CCR5 binding in the absence of sCD4 (*13*). None of the peptides, including 12p1, were able to inhibit binding of sCD4 to the S375W trimeric envelope glycoprotein (Figure 6B).

Localization of Peptide Binding. In an effort to further elucidate the nature of the binding of 12p1 to gp120, we used a modification of the ELISA described above to

determine peptide competition with a panel of human anti-gp120 mAbs. Peptide and antibody were added to the immobilized trimers simultaneously, and bound antibody was detected with an HRP-conjugated goat anti-human antibody. Figure 7A shows the binding of four different antibodies to the envelope glycoprotein trimers in the absence or presence of peptides 12p1 and [R1A]12p1. Antibody 2G12 recognizes a discontinuous glycosylated epitope in the gp120 outer domain (*14−16*). The 17b antibody, which recognizes an epitope overlapping the CCR5 binding region (*17*), is the same CD4-inducible antibody used in the biosensor experiments. Antibodies F105 and b12 both bind distinct epitopes overlapping the CD4 binding site (*18−20*). However, F105 preferentially binds an unactivated, or CD4-unbound, conformation of gp120 (*13*).

With wild-type envelope glycoprotein trimers, antibodies 2G12 and b12 bound well, and the peptides did not affect this binding. 12p1 inhibited the binding of both 17b, as was seen in Figure 1B, and F105. [R1A]12p1 slightly inhibited these interactions as well, but was much less effective. Identical experiments were performed with two mutant envelope glycoprotein trimers with changes in gp120. The S375W variant, as described earlier, favors the CD4-bound, "active", conformation, while I423P disrupts the CD4-bound conformation (*13*). As seen in Figure 7B, each antibody in the absence of peptide bound similarly to the S375W and wt trimers, except for F105. This result is consistent with previous studies suggesting that F105 favors an "unactivated" conformation of gp120 and that the S375W mutant approximates a more "activated", CD4-bound conformation (*4, 13*). Neither peptide inhibited the binding of 17b to the S375W trimer.
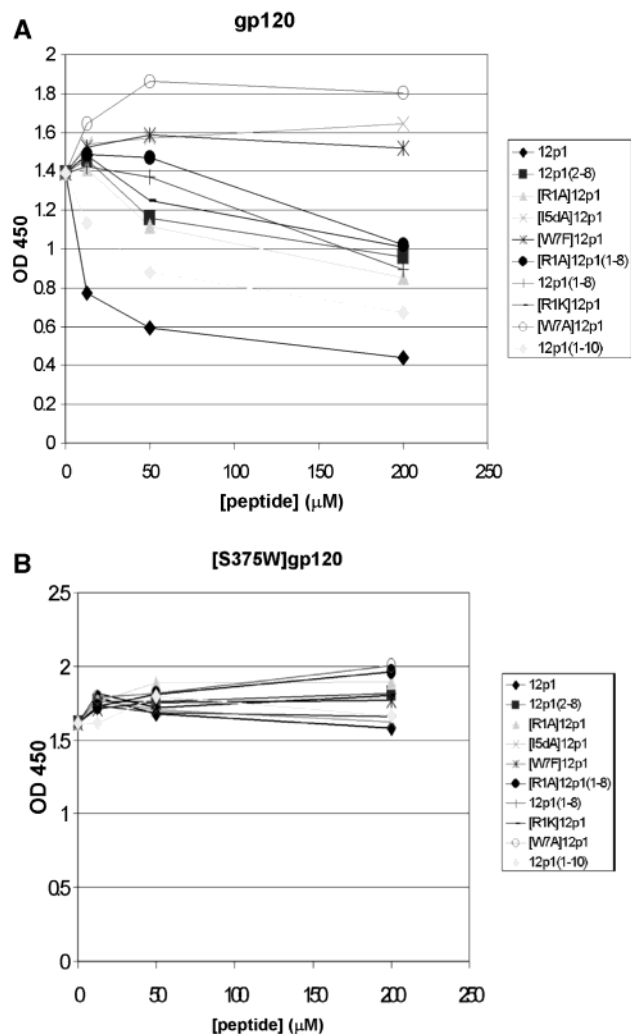
FIGURE 6: Effects of peptides on CD4 interaction with wild-type (A) and S375W mutant (B) envelope glycoprotein trimers. Soluble trimers of wild-type or S375W envelope glycoproteins were immobilized on ELISA plates. Peptides at varying concentrations were incubated with biotinylated sCD4 and added to the plates. The extent of sCD4 binding was assessed with avidin-bound HRP.

The I423P mutant does not bind CD4 or 17b and is thought to be inefficient at assuming the CD4-bound conformation (*13*). Here, I423P trimers bound 2G12 and b12 as well as the wild-type gp120, and 12p1 did not significantly affect antibody binding (Figure 7C). 17b did not bind to this "unactivated" gp120 mutant, as previously reported (*13*). F105, however, was able to bind I423P trimers very well, and peptide 12p1 inhibited the interaction.

Effects of the Peptide on gp120−CCR5 Interactions. As 12p1 inhibits interactions of gp120 with both CD4 and 17b, we sought to determine if the inhibitory effect on 17b, a CCR5 surrogate, could be extended to CCR5 itself. To test this, we studied the binding of a CD4-independent gp120 (ADA ΔV1/V2) metabolically labeled with [^{35}S]Cys/Met, in the presence or absence of peptides, to CD4-negative target Cf2Th cells expressing CCR5 (*21*). The bound proteins were immunoprecipitated with a mixture of sera from HIV-1-infected individuals and visualized by SDS−PAGE. Figure 8 shows a hierarchy of CCR5 inhibition efficacies similar to that obtained with the biosensor and ELISA for CD4 and 17b inhibition. 12p1 strongly inhibited binding of gp120 to CCR5, with the other peptides exhibiting reduced activity.
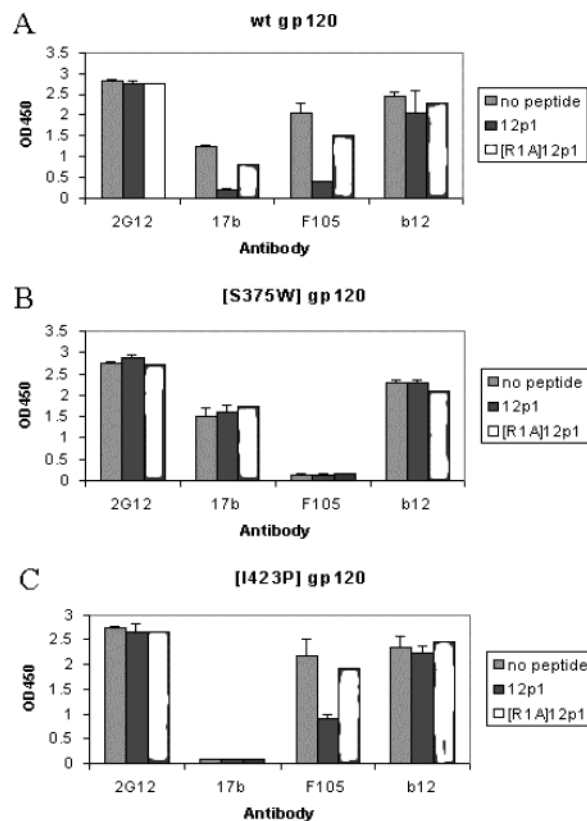

FIGURE 7: Inhibition of binding of antibodies to immobilized wild-type (A), S375W (B), and I423P (C) envelope glycoprotein trimers. Wild-type or mutant envelope glycoprotein trimers were captured on ELISA plates. Different antibodies to gp120 were incubated with or without peptide (100 μM), and then added to the plates. The extent of antibody binding was measured with HRP-conjugated secondary Ab.
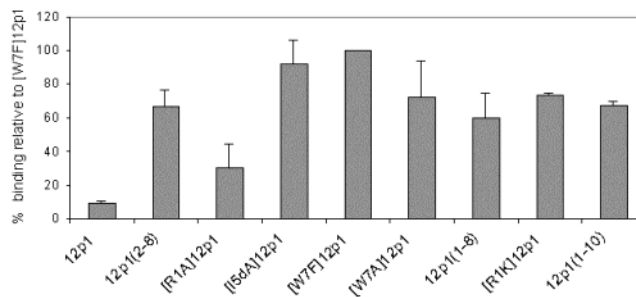

FIGURE 8: Peptide inhibition of binding of gp120 to cell surface CCR5. The ADA ΔV1/V2 gp120 glycoprotein was incubated with the various peptides (100 μM), and then added to Cf2Th cells expressing CCR5. Bound proteins were precipitated, and the extent of peptide inhibition was determined.

The one exception to the above correlation is peptide [R1A]12p1, which exhibited strong inhibition of CCR5 binding, but had levels of 17b and CD4 inhibition much lower than that of 12p1.

Peptide Inhibition of Viral Infection. To determine whether 12p1 inhibits infection of cells by HIV-1 virus, we used a single-round infection assay in which recombinant HIV-1 viruses encoding luciferase are pseudotyped with different envelope glycoproteins. The 12p1 peptide was incubated with recombinant wild-type and mutant viruses, and this virus/peptide mixture was added to target cells expressing the appropriate HIV-1 receptors. The luciferase activity in the cells provided an indication of the efficiency of infection in
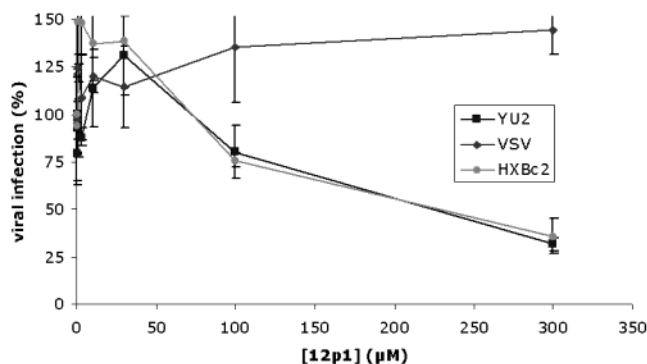
FIGURE 9: Inhibition of viral infection by 12p1. Single-round, replication-defective viruses, displaying envelope glycoproteins of VSV or HIV-1 isolates (YU2 or HXBc2) and containing a firefly luciferase reporter gene, were incubated with 12p1 (0.3−300 μM) at 37 °C for 30 min. Cf2Th-CD4-CCR5 target cells were then incubated with the virus−peptide mixture for 48 h at 37 °C. Viral infection was detected by cell lysis, followed by the measurement of luciferase activity. Data are reported as the percentage of viral infection in the absence of the peptide.

the presence of the peptide. 12p1 inhibited infection of cells by both R5 (YU2, JR-CSF, and ADA) and X4 (HxBc2) HIV-1 isolates (Figure 9 and data not shown). The observed inhibition was specific to HIV, as infection with a VSV G-pseudotyped control virus was not inhibited.

The inhibition of several variants of the ADA, YU2, and JR-CSF viruses by 12p1 was examined. In CD4-CCR5-expressing target cells, 12p1 was found to have IC_{50} values of 8 μM for wild-type ADA and 67 and 90 μM for the CD4-independent [N197S]gp120 and ADA ΔV1/V2 viruses, respectively (data not shown). The 12p1 peptide did not inhibit infection of cells by virus pseudotyped with YU2 [S375W] envelope glycoproteins (data not shown), in agreement with the trimer ELISA data (Figure 6). Finally, while cell infection by a virus pseudotyped with wild-type JR-CSF envelope glycoprotein was inhibited by 12p1, a variant in which Arg476 substituted with Ala was strongly resistant to 12p1 (Figure 10A). Similar substitutions at residues Lys97 and Glu102 showed intermediate resistance (data not shown). These gp120 residues are located near the binding site for CD4 (Figure 10B) but do not make contact with CD4 (*12*).

DISCUSSION

The overall goal of this study was to gain an improved understanding of the properties governing the interaction of peptide 12p1 (RINNIPWSEAMM) with HIV-1 gp120 and, by inference, how it is able to inhibit binding interactions of the multiple function-associated receptor with gp120. We used SPR to quantitate 12p1 binding. We showed that 12p1 inhibits YU2 gp120 binding to both CD4 and 17b with equivalent potencies, with IC_{50} values of 1.1 and 1.6 μM, respectively (Figure 1). 12p1 inhibition of CD4 binding was found to be noncompetitive (Figure 4), possibly caused by allosteric binding of the peptide to gp120 at a site present in the CD4-unbound form of gp120 that lies adjacent to the site of the CD4 binding footprint (Figure 10B). Importantly, 12p1 inhibition of CD4 and 17b binding (Figures 6A and 7A) was found to extend to trimeric envelope glycoproteins of the HxBc2 strain, a prerequisite for inhibitors targeted to multiple and diverse viral isolates. The IC_{50} versus CD4 estimated for the trimer using the ELISA (12.5 μM) was
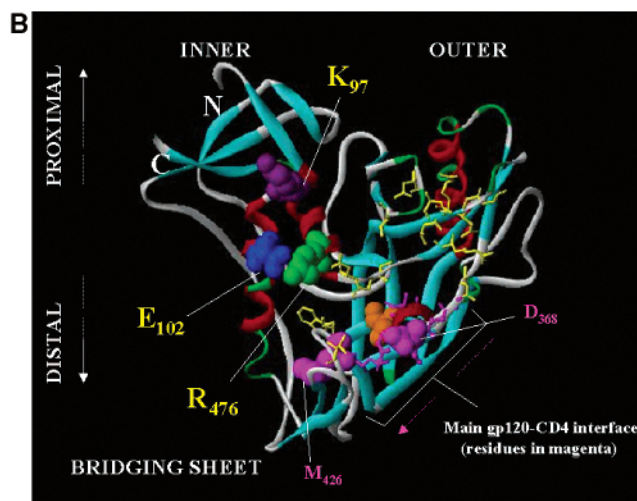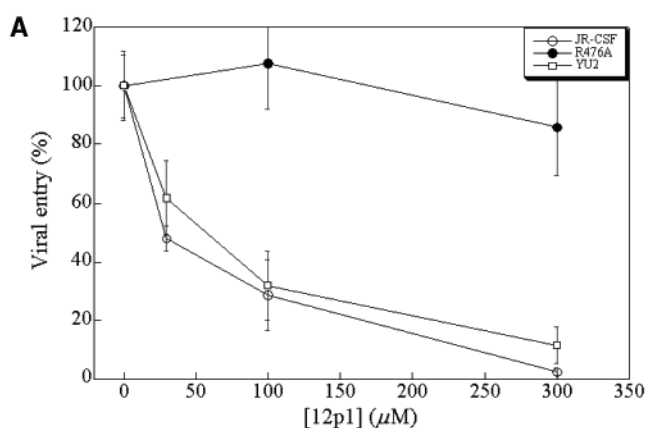

FIGURE 10: (A) 12p1 inhibition of infection by JR-CSF viruses pseudotyped with envelope variants. The recombinant HIV-1 viruses (JR-CSF) expressing firefly luciferase and containing the wild-type and mutant envelope glycoproteins were used to infect Cf2Th-CD4-CCR5 cells in the presence of different concentrations of 12p1. The percentage of luciferase measured in the target cells relative to that in the absence of 12p1 is shown. The values are the means and standard deviations of triplicate points in the assay, and results are typical of those obtained in two independent experiments. (B) Structural localization of residues whose mutations lead to decreased 12p1 efficacy. The crystal structure of wild-type YU2 core gp120 is shown in ribbon format and colored on the basis of secondary structure: red for α-helix, blue for β-sheet, green for turns, and white for unordered. Labeled in yellow are residues that contact CD4 as determined by Kwong et al. (*12*), whereas residues in magenta are amino acids that form the CD4−gp120 interface (CD4 Phe43 binding pocket). The important Ser375 is shown in orange. As can be seen, the three residues which when mutated weaken the 12p1 inhibitory effect (K97, E102, and R476) reside in a locale distinct but adjacent to residues involved in CD4 binding. This area could potentially be involved in 12p1 binding.

slightly higher than that suggested by the SPR data (not shown). The difference in IC_{50} may reflect differences between monomeric and trimeric forms of the HIV-1 envelope glycoproteins, between the methods, or between the two gp120 strains. The possibility of strain disparity was expected, however, as 12p1 was previously reported to have slightly different efficacies against gp120s derived from different viral strains (*7*).

A key aim of this study was to determine the stoichiometry of binding of 12p1 to gp120, as this had not been addressed before and the potential usefulness of the peptide as an antagonist lead depends on a well-defined stoichiometry for

binding to gp120. Figure 2 shows that 12p1 indeed binds directly to gp120, and that the extent of this binding is concentration-dependent. Over the range of concentrations at which 12p1 inhibits binding of gp120 to CD4, 17b, and CCR5, the interaction appears to occur with a binding stoichiometry of ≤1:1. Although we did see interactions at the highest concentrations of peptide that might fractionally exceed 1:1 binding, these may be due to peptide aggregating with itself. There is no evidence for a >1:1 stoichiometry at the lowest concentrations, where inhibition is still very strong. In addition, the observation that 12p1 inhibits CD4 and 17b binding with nearly identical IC_{50} values supports a single binding site for the peptide. Considering all these data, we conclude that the binding interaction of 12p1 with gp120 is specific and leads to a 1:1 peptide−gp120 complex. This finding strongly argues for a unique 12p1 binding site and predicts the possibility of using 12p1 structure in the gp120-bound state as a template for the design of novel CD4−gp120 antagonists.

Another key aim of this investigation was to determine whether the peptide binds in a manner similar to that of CD4 or by an alternative mechanism. The two most critical gp120 binding residues on CD4 are Phe43 and Arg59 (*12*, *22*). The presence of the large aromatic residue Trp, along with the Arg at the N-terminus of 12p1, led us to consider the possibility that the peptide mimics CD4 binding. Making this possibility more likely is the presence of Pro6, which could promote formation of a turn at the Trp7 position that would be analogous to the β-turn containing the critical Phe43 of CD4. The first logical peptide variation, then, was to replace Trp7 with Phe. Ferrer and Harrison had previously reported that Ala could not substitute for Trp in the peptide (*7*), but we found also that Phe cannot replace the Trp residue. [W7F]12p1 did not inhibit CD4 or 17b binding (Figure 6 and data not shown). Direct binding studies showed that [W7F]12p1 was able to bind to gp120, but the level of binding was very low at high peptide concentrations (not shown). Since Phe is not a surrogate for Trp7 and 12p1 has a much different effect on gp120 than does CD4, it is likely that the peptide does not bind to gp120 in the same manner as CD4. Nonetheless, a binding site near the CD4 site remains possible and even likely (see below).

Our data also confirm that the entire sequence of 12p1 is important for its action. A change of Arg1 to Ala or Lys caused a reduction in inhibitory activity, but not complete loss of inhibition (Figures 5 and 6). The various truncations of 12p1, from either the N- or C-terminal end, also reduced the efficacy of the peptides (Figures 5 and 6). In these cases, the truncations did not seem to affect the mode of action of the peptides, but seemed instead to have reduced their affinities for gp120, as demonstrated by direct binding experiments with these peptides (data not shown). A peptide smaller than residues 2−8 was not tested, as it was previously shown that these internal residues were critical for peptide activity (*7*). The other peptide besides [W7F]12p1 with a mutation in one of these interior residues, [I5dA]12p1, also lost all inhibitory activity toward gp120 binding (Figure 6). The D-Ala residue was meant to disrupt the backbone structure of the peptide, perhaps interfering with a possible turn, indicated by the presence of the neighboring Pro residue. It is not known if indeed a turn is formed by the peptide after it binds to gp120, but the D-Ala in place of

Ile5 likely would alter the conformation of the original 12p1 peptide. The importance of peptide conformation is unclear, however, as replacement of Ile5 with L-Ala also reduced inhibitory activity (*7*). We conclude from the available sequence variation data that many of the interior 12p1 sequence elements, and possibly peptide conformation, are critical for 12p1 inhibition of gp120 binding interactions, while the more distal residues may enhance peptide binding affinity.

A noteworthy property of 12p1 elucidated in the original report of Ferrer and Harrison (*7*) is the concomitant inhibition of binding of gp120 to 17b and CD4. No other peptide inhibitors of gp120−CD4 binding that have been identified so far inhibit binding of both ligands (*1*, *5*, *6*). In the current work, we demonstrated that the inhibitory effect of the peptide extends to the coreceptor CCR5, therein showing that the peptide suppresses binding to both envelope receptors of the host cell. Assays of binding of gp120 to cells expressing CCR5 on their surface in the absence of CD4 showed that 12p1 could indeed inhibit this interaction (Figure 8). Only ~10% of the gp120 was able to bind to CCR5 on the cells in the presence of 12p1, compared with binding in the presence of [W7F]12p1. The other peptide variants were much less able to inhibit this binding, except for [R1A]12p1, which did show significant inhibition. These data demonstrate that the effects of 12p1 are not confined to *in vitro* receptor surrogates. The additional ability of 12p1 to inhibit viral infection of cells (Figure 9) supports its possible value as a therapeutic lead.

The demonstration that 12p1 inhibits recognition of both host cell receptors by the envelope protein, combined with elucidation of both 1:1 stoichiometry and a non-CD4 character of peptide sequence usage, evokes the enticing possibility of designing unique antagonists of the HIV-1 fusion process. Toward that objective, it will be important to delineate the mechanism of action of 12p1. Several types of data obtained in this work provide key starting points in achieving this goal. CD4 saturation competition binding analysis (Figure 4) suggests that the inhibition of CD4 binding by 12p1 is noncompetitive. This argues that 12p1 is not binding at the same binding site as CD4. The findings with escape variants (for example, Figure 10A) give structural support to this latter conclusion. These results identify residues 97, 102, and 476 as being potentially important in 12p1 binding. None of these residues are CD4 contacts (*12*), although they are near the CD4 binding site (Figure 10B). That residues 97, 102, and 476 involve both the inner and outer domains of gp120 leaves open the possibility that 12p1 inserts into an interdomain interface on unliganded gp120. Of note here is also the fact that residues E102 and R476 are conserved among all HIV-1 isolates (*12*), which implies that peptide 12p1, or derivatives thereof, may prove to be effective against a broad range of viral isolates across multiple clades.

Other binding data in this work further clarify the nature of the 12p1 binding site. Because 12p1 is effective on trimeric and functional envelope glycoproteins, as well as gp120 monomers, we can rule out interactions with the portions of gp120 that are inaccessible on the trimer, primarily the inner domain (*23*). The 2G12 antibody recognizes a largely glycosylated (mostly mannose) gp120 epitope specified by the C3 and V4 regions (*14*−*16*). 2G12 can bind
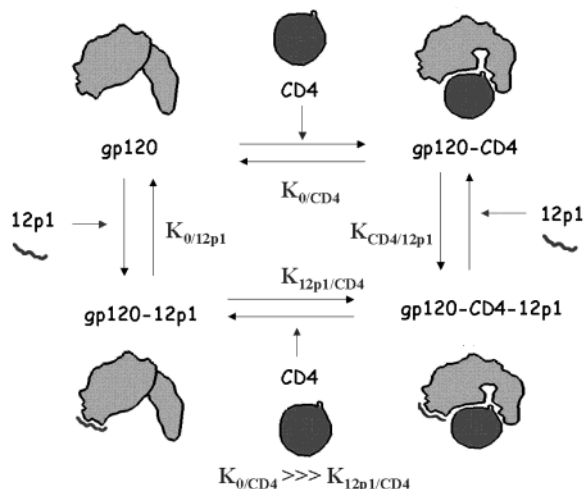
FIGURE 11: Scheme showing a proposed allosteric model for the mode of inhibition of gp120 by 12p1. In this model, gp120 is assumed to exist in at least two distinct forms: (1) a CD4 binding efficient form and (2) a CD4 binding inefficient form. gp120 in both states can bind to the 12p1 inhibitor, but the latter binds preferentially to the inefficient form (left side of the diagram). The binding of 12p1 to gp120 is proposed to "trap" a conformational state that CD4 cannot access and that exhibits slow refolding kinetics back to a CD4 binding efficient conformation.

gp120 in multiple conformations. The 12p1 peptide had no effect on 2G12 binding, and thus, the peptide is not interacting with that glycosylated epitope. The interrelationship of 12p1 and Ab b12 is slightly unusual. Since b12 is a CD4 binding site (CD4BS) Ab and the peptide does not compete with it, we might conclude that the peptide does not bind to the CD4 binding site. The b12 epitope, however, seems to be dependent on the gp120 strain and/or oligomerization state. Xiang et al. (*13*) found that b12 did not bind to monomers of S375W from the YU2 strain, while here we found robust binding to HXBc2 trimers and mutants. This may be due to the importance of the V1 and V2 loops of gp120, which vary among strains, for b12 recognition, and also to the differences between the monomer and trimer. Whatever the b12 epitope, it does not appear to overlap significantly with the binding site of the 12p1 peptide. Further support for this assumption comes from a recent study (*24*), which shows that b12 is only moderately affected by alanine substitutions of E102 and R476. The ability of 12p1 to inhibit binding of F105, another CD4BS Ab, might be due to epitope overlap, the common effect of unactivated state binding, or both.

That 12p1 appears to bind at a site different from that of CD4 leads us to the hypothesis that this peptide functions allosterically and inhibits envelope interactions with its receptors by stabilizing a conformational state closer to that of unliganded gp120 rather than the activated, CD4-bound form (Figure 11). Because gp120 in its unliganded form is highly flexible (*1*), it is likely that it exists in a range of conformations between its unliganded state and activated state. In accordance with this view, peptide 12p1 could either stabilize a nonproductive intermediate conformation of gp120 or prevent the transition to an active conformation of gp120. Several types of data obtained in this work are consistent with the view described above. 12p1 does not inhibit binding of CD4 to the gp120 variant S375W, which is believed to be in a ligand-activated state (*4, 13*), suggesting that 12p1

cannot access this latter state. In contrast, 12p1 inhibits binding of F105 to the I423P variant of envelope trimers, suggesting that 12p1 can access the unactivated state that this envelope mutant assumes and hence could stabilize an unactivated state in the HIV-1 envelope. These data are consistent with the possibility that the HIV-1 envelope may not be able to convert to a conformation that is appropriate for high-affinity receptor binding once 12p1 is bound.

In this work, we determined that peptide 12p1 inhibits the interaction of gp120 with both CD4 and 17b with similar IC_{50} values. The inhibition extends to different strains of gp120, to both monomers and trimers, and to cellular coreceptor CCR5. 12p1 also is able to inhibit viral infection of cells. Several sequence elements, as well as the length of the peptide, are critical for its effectiveness. Truncations of the peptide and changes in residues 2−8 all caused reduction in inhibitory activity. 12p1 appears to bind preferentially to an unactivated conformation of gp120 to which CD4 and 17b/CCR5 are unable to bind, thereby inhibiting viral infection. Dual inhibition of CD4 and coreceptor binding and inhibition of viral infection evoke the enticing possibility of using 12p1 as an HIV/AIDS therapeutic lead. In this regard, the data obtained in this work show clearly that 12p1 binds in a 1:1 manner at a unique site on gp120 that can be distinguished from that of CD4 or the coreceptor. This now raises the possibility of determining the structure of 12p1 in the bound state and using that structure to design higher-affinity antagonists. Since 12p1 itself already has a substantial (low micromolar K_D) affinity even without the conformational constraint and alternative scaffolding that could be employed in follow-ups, the results of this work allow the chance of utilizing this peptide system in the drug discovery process.

REFERENCES

1. Dowd, C. S., Leavitt, S., Babcock, G., Godillot, A. P., Van Ryk, D., Canziani, G. A., Sodroski, J., Freire, E., and Chaiken, I. M. (2002) *Biochemistry 41*, 7038−7046.

2. Myszka, D. G., Sweet, R. W., Hensley, P., Brigham-Burke, M., Kwong, P. D., Hendrickson, W. A., Wyatt, R., Sodroski, J., and Doyle, M. L. (2000) *Proc. Natl. Acad. Sci. U.S.A. 97*, 9026−9031.

3. Kwong, P. D., Doyle, M. L., Casper, D. J., Cicala, C., Leavitt, S. A., Majeed, S., Steenbeke, T. D., Venturi, M., Chaiken, I., Fung, M., Katinger, H., Parren, P. W., Robinson, J., Van Ryk, D., Wang, L., Burton, D. R., Freire, E., Wyatt, R., Sodroski, J., Hendrickson, W. A., and Arthos, J. (2002) *Nature 420*, 678−682.

4. Raja, A., Venturi, M., Kwong, P., and Sodroski, J. (2003) *J. Virol. 77*, 713−718.

5. Vita, C., Drakopoulou, E., Vizzavona, J., Rochette, S., Martin, L., Menez, A., Roumestand, C., Yang, Y. S., Ylisastigui, L., Benjouad, A., and Gluckman, J. C. (1999) *Proc. Natl. Acad. Sci. U.S.A. 96*, 13091−13096.

6. Li, C., Dowd, C. S., Zhang, W., and Chaiken, I. M. (2001) *J. Pept. Res. 57*, 507−518.

7. Ferrer, M., and Harrison, S. C. (1999) *J. Virol. 73*, 5795−5802.

8. Yang, X., Farzan, M., Wyatt, R., and Sodroski, J. (2000) *J. Virol. 74*, 5716−5725.

9. Farzan, M., Mirzabekov, T., Kolchinsky, P., Wyatt, R., Cayabyab, M., Gerard, N. P., Gerard, C., Sodroski, J., and Choe, H. (1999) *Cell 96*, 667−676.
10. Parolin, C., Taddeo, B., Palu, G., and Sodroski, J. (1996) *Virology 222*, 415−422.
11. Rho, H. M., Poiesz, B., Ruscetti, F. W., and Gallo, R. C. (1981) *Virology 112*, 355−360.
12. Kwong, P. D., Wyatt, R., Robinson, J., Sweet, R. W., Sodroski, J., and Hendrickson, W. A. (1998) *Nature 393*, 648−659.
13. Xiang, S. H., Kwong, P. D., Gupta, R., Rizzuto, C. D., Casper, D. J., Wyatt, R., Wang, L., Hendrickson, W. A., Doyle, M. L., and Sodroski, J. (2002) *J. Virol. 76*, 9888−9899.
14. Sanders, R. W., Venturi, M., Schiffner, L., Kalyanaraman, R., Katinger, H., Lloyd, K. O., Kwong, P. D., and Moore, J. P. (2002) *J. Virol. 76*, 7293−7305.
15. Scanlan, C. N., Pantophlet, R., Wormald, M. R., Ollmann Saphire, E., Stanfield, R., Wilson, I. A., Katinger, H., Dwek, R. A., Rudd, P. M., and Burton, D. R. (2002) *J. Virol. 76*, 7306−7321.
16. Trkola, A., Purtscher, M., Muster, T., Ballaun, C., Buchacher, A., Sullivan, N., Srinivasan, K., Sodroski, J., Moore, J. P., and Katinger, H. (1996) *J. Virol. 70*, 1100−1108.
17. Thali, M., Moore, J. P., Furman, C., Charles, M., Ho, D. D., Robinson, J., and Sodroski, J. (1993) *J. Virol. 67*, 3978−3988.
18. Thali, M., Olshevsky, U., Furman, C., Gabuzda, D., Posner, M., and Sodroski, J. (1991) *J. Virol. 65*, 6188−6193.
19. Burton, D. R., Pyati, J., Koduri, R., Sharp, S. J., Thornton, G. B., Parren, P. W., Sawyer, L. S., Hendry, R. M., Dunlop, N., Nara, P. L., et al. (1994) *Science 266*, 1024−1027.
20. Roben, P., Moore, J. P., Thali, M., Sodroski, J., Barbas, C. F., III, and Burton, D. R. (1994) *J. Virol. 68*, 4821−4828.
21. Kolchinsky, P., Kiprilov, E., Bartley, P., Rubinstein, R., and Sodroski, J. (2001) *J. Virol. 75*, 3435−3443.
22. Moebius, U., Clayton, L. K., Abraham, S., Diener, A., Yunis, J. J., Harrison, S. C., and Reinherz, E. L. (1992) *Proc. Natl. Acad. Sci. U.S.A. 89*, 12008−12012.
23. Kwong, P. D., Wyatt, R., Sattentau, Q. J., Sodroski, J., and Hendrickson, W. A. (2000) *J. Virol. 74*, 1961−1972.
24. Pantophlet, R., Ollmann-Saphire, E., Poignard, P., Parren, P. W., Wilson, I. A., and Burton, D. R. (2003) *J. Virol. 77*, 642−658.

BI035088I